Magn Reson Mater Phy (2012) 25:113–126
DOI 10.1007/s10334-011-0298-z

RESEARCH ARTICLE

Magnetisation transfer effects of Q2TIPS pulses in ASL

Enrico De Vita · Matthias Günther · Xavier Golay · David L. Thomas

Received: 19 July 2011 / Revised: 11 October 2011 / Accepted: 1 December 2011 / Published online: 28 December 2011

Abstract
Object In pulsed arterial spin labelling (ASL), Q2TIPS saturation pulses are used to actively control the temporal width of the labelled bolus. However, these Q2TIPS pulses also induce magnetisation transfer (MT) effects in the adjacent tissue. In this work, we investigated how Q2TIPS-related MT alters tissue signal in pulsed ASL and, consequently, CBF quantification.
Materials and methods Seven volunteers were studied at 3 tesla using a multi-TI FAIR sequence and 3D-GRASE readout with background suppression. Q2TIPS pulses were used and the spacing between RF pulses was varied to modulate MT effects. Computer simulations were designed to mimic in-vivo signals at multiple TI values.
Results Q2TIPS-associated MT was found to reduce tissue T1 and M0 values by up to 42 and 50% respectively; leading to a reduction of up to 40% in the effectiveness of background suppression and, therefore, increased sensitivity to motion for the longest TI values. In addition, greater MT effects were associated with reduced grey matter CBF estimates of up to 15%.
Conclusions The MT effect associated with the Q2TIPS pulse train has a significant effect on tissue signal. It is recommended that MT effects are characterised and both background suppression and Q2TIPS schemes are accordingly optimised to reduce the effects of MT on accuracy and precision of CBF estimation.

Keywords Brain/blood supply · Cerebrovascular circulation/physiology · Humans · Magnetic resonance imaging/methods · Spin labels

E. De Vita (✉) · X. Golay
Lysholm Department of Neuroradiology, National Hospital for Neurology and Neurosurgery, University College London Hospitals NHS Foundation Trust, Queen Square, Box 65, London WC1N 3BG, UK
e-mail: edevita@medphys.ucl.ac.uk

E. De Vita · X. Golay · D. L. Thomas
Academic Neuroradiological Unit, Department of Brain Repair and Rehabilitation, UCL Institute of Neurology, Queen Square, London WC1N 3BG, UK

M. Günther
Mediri GmbH, Heidelberg, Germany

M. Günther
Fraunhofer MEVIS-Institute for Medical Image Computing, Bremen, Germany

M. Günther
Faculty for Physics and Electrical Engineering, University Bremen, Bremen, Germany

Introduction

Non-invasive brain perfusion measurements with arterial spin labelling (ASL) sequences are becoming increasingly popular and are now being commercialized by all main scanner manufacturers as complementary or alternative methods to dynamic susceptibility contrast (DSC) measurements based on injection of gadolinium-containing contrast agents.

In perfusion quantification with ASL, the delay between the application of the tag and arrival of the tagged blood in the tissue (typically referred to as either transit time, arterial arrival time, or bolus arrival time, BAT) is a potential source of systematic error, because it varies widely across individuals and brain regions [1].

Wong et al. [2] introduced a modification of the pulsed ASL (PASL) scheme to make the technique relatively insensitive to BAT by controlling the time duration of the

tagged bolus using an additional saturation pulse (QUIPSS II). The Q2TIPS approach [3] provided further improvements in terms of reduced sensitivity to B1 inhomogeneity and a better match of the slice profiles of the saturation and labelling pulses: the trailing edge of the inverted blood bolus is sharply truncated at a defined time (TI1) by applying a series of spatially selective pulses designed to efficiently saturate the flowing blood signal over a thin-slice region proximal to the imaging area.

In principle, the use of Q2TIPS enables estimation of CBF on the basis of a measurement at a single post-labelling delay time (TI). However, the effectiveness of Q2TIPS depends on BAT values being within a specific range, and this assumption may be violated in some neurovascular diseases with late arrival times, compromising the accuracy of CBF estimates.

A more robust approach to CBF estimation consists in acquiring ASL images over a range of TI values [4–6]. By using a fast readout scheme, it becomes feasible to collect multi-TI data in a reasonable acquisition time, enabling simultaneous estimates of local CBF and BAT using Buxton's general kinetic model [7]. This makes ASL more suitable for full characterisation of cerebral haemodynamics in response to pathology, drugs, or physiological challenges [8]. However, even with this multi-TI approach, it is still useful to use Q2TIPS saturation pulses for the longest TI acquisitions, in order to truncate the trailing edge of the tagged bolus. This enables accurate definition of its temporal width and facilitates CBF quantification.

In addition, background suppression (BS) of static tissue is also normally used to improve the temporal stability of the difference images and, therefore, reduce the variance in the CBF measurements [9]. Detection of the small ASL signal is extremely sensitive to changes in background tissue signal, because of unwanted motion or physiological noise. In principle it would be beneficial to have zero signal from static tissue at any TI. When a BS scheme is used, a number of inversion pulses are used to suppress static tissue when the readout pulse is applied [9]. In practice the BS scheme is often set up to generate a null signal some time before the excitation pulse to avoid negative magnetisation and enable magnitude reconstruction. In this case the ideal situation is to have the same (small) static tissue signal at all TI values.

Magnetisation transfer (MT) effects associated with the ASL labelling pulses have been fully characterised, and have led to the development of an array of ASL labelling schemes designed to balance MT effects between labelling and control experiments, or to make MT-related effects negligible [10, 11]. However, as far as we are aware there has been no published investigation of the effects of the RF power associated with the Q2TIPS pulse train, which will also induce an associated MT effect. In addition to saturating blood water in the tagging region, the Q2TIPS pulse train is likely to reduce tissue and blood signals in the imaging volume via direct saturation and true magnetisation transfer related to their macromolecular pool fraction (these effects will be hereafter indicated together as simply the "MT effect").

In this work, we examine this unintended effect of the Q2TIPS pulses on the perfusion-weighted ASL signal. By using a multi-TI PASL protocol with BS, we explore how the Q2TIPS-related MT effect:

1. alters the effective tissue T1 and therefore the efficiency of suppression of static tissue signal, with the associated effect on the precision/sensitivity to temporal instabilities of the perfusion measurement [9]; and
2. can influence the estimation of quantitative CBF values.

Materials and methods

Subjects and main MR acquisition protocol

Data were acquired on a 3T Siemens TIM Trio using a body coil RF transmitter and a 32-channel head-coil receiver. Seven healthy volunteers were scanned after giving informed consent, in accordance with the local research ethics protocol.

The PASL sequence used the FAIR tagging scheme [12, 13], a single-shot 3D-GRASE readout [14], and Q2TIPS [3] for definition of the tagged bolus duration; a BS scheme was also implemented [9].

The 3D-GRASE readout (bandwidth 2,790 Hz/pixel) used GRAPPA [15] with acceleration factor 2 in the phase encode (PE) direction resulting in the acquisition of 21 PE lines (axial in-plane image matrix 64 (readout direction) × 36 (PE)) and 24 6 mm thick partitions (6/8 partial Fourier) in the head-feet (z) direction, with a field of view 288 mm × 162 mm. The resulting nominal resolution was $4.5 \times 4.5 \times 6$ mm^3. The echo time (TE)/repetition time (TR) was 15/3,300 ms. Two averages were used throughout for a total acquisition time of 3 min 8 s. A fat-saturation pulse was also used. A diagram of the sequence (except for the pre-saturation scheme played out before the inversion pulse) can be seen in Fig. 1 of Ref. [14].

Image volume pre-saturation (nominal slab thickness 150 mm) used the same parameters as in Ref. [16]; in brief, pre-saturation used a 4-pulse WET scheme with optimised flip angles, inter-pulse duration (10 ms) and an adjustable delay just before the inversion pulse (optimised to 15 ms); post-inversion saturation was provided by a single 90° pulse.

The inversion pulses for both tagging and BS were 10.2 ms C-shape FOCI pulses [17] (FOCI factor 2, $\beta = 12$ s^{-1}, $\mu = 800$). The tagging pulses were played out

with (Ss) and without (Ns) slice selection gradients for control and tag acquisitions respectively.

Two non-selective BS pulses were used and the timing of their application was calculated analytically for each TI to best minimise signals with T1 = 700 ms and 1,400 ms (roughly corresponding to tissue T1s at 3T [18]) 100 ms before the excitation pulse for the readout, as in Ref. [14]. The post-labelling delay TI was varied from 300 to 2,700 ms in 200-ms steps. For Q2TIPS 5.12 ms sinc-shaped pulses (1,500 Hz bandwidth), cosine modulated at 3 kHz to produce saturation bands (of 40 mm thickness) on either side of the imaging slab, were used (as in Ref. [14]). The interval between successive pulses was 9 ms, during which time crusher gradients were applied.

Measuring the effect of reducing the density of the saturation pulses used for Q2TIPS

To investigate the MT effect associated with the Q2TIPS module, the density of the Q2TIPS pulse train was varied. By reducing the pulse density, the mean deposited RF power is reduced, and so the associated MT effect is also reduced. Pulse density reduction was implemented by setting the amplitude of some of the Q2TIPS pulses to zero.

It is possible to calculate a cut-off velocity v_c associated with the Q2TIPS pulses, as done by Luh et al. [3]. For the original Q2TIPS pulse density we calculated $v_c \approx 280$ cm/s.

Because 80–100 cm/s is likely to be sufficient to saturate flowing blood, we reduced the cut-off velocity by 1/2 or by 2/3 and compared the results with those obtained by use of the original "standard" saturation scheme; this resulted in 3 different procedures:

1. back-to-back saturation pulses are played out (minimum inter-pulse delay; henceforth referred to as Sat1/1);
2. in the Q2TIPS Sat1/2 scheme, only every other pulse is played out (resulting in $v_c \approx 140$ cm/s);
3. in the Q2TIPS Sat1/3 scheme, only every third pulse has non-zero amplitude (resulting in $v_c \approx 93$ cm/s).

All of the spoiler gradients of the "standard" Q2TIPS procedure (occurring between each pair of RF pulses) were played out irrespective of the chosen scheme.

Measuring the MT effect of the Q2TIPS module without truncating the bolus

To measure the MT effect of the saturation pulses without affecting the tagged bolus, an extra option was introduced in the sequence to play out the Q2TIPS pulse train *without* the slice-selection gradients that define the saturation slabs; this is referred to as *NoGrads*. In so doing, the saturation pulses are off-resonance for the whole volume of interest (imaging slab and previously defined saturation bands also) and will *not* result in truncation of the trailing edge of the tagged bolus. They should, however, produce the equivalent MT effect on the imaging slab and on the flowing blood, much as in the control phase of the PICORE ASL tagging scheme [19]. Measurements were made with this NoGrads option using the Sat1/1 Q2TIPS scheme and TI1 = 500 ms.

Measuring tissue M0 and T1, $M0_{Sat}$ and $T1_{Sat}$

To measure tissue M0 and T1, the BS pulses were turned off (NoBS) and data collected with increasing TI. Because there is a saturation pulse immediately after the inversion pulse, this is equivalent to a saturation recovery experiment. The results obtained with Ss data are used for the analysis in this paper. Completely analogous results (within 1%) were obtained using the Ns data (data not shown).

To measure the reduced apparent M0 and T1 due to Q2TIPS-related MT effect, $M0_{Sat}$ and $T1_{Sat}$, the Q2TIPS pulse train was started immediately after the post-inversion saturation pulse (i.e. TI1 = 0 ms). Similarly $M0_{Sat}$ and $T1_{Sat}$ were measured for the Q2TIPS Sat1/2 and Sat1/3 schemes, to yield $M0_{Sat1/2}$, $T1_{Sat1/2}$, $M0_{Sat1/3}$, $T1_{Sat1/3}$. For one subject, $M0_{Sat1/1\text{-NoGrads}}$ and $T1_{Sat1/1\text{-NoGrads}}$ were also measured without application of the slice-selection gradients with the standard Sat1/1 Q2TIPS procedure.

Data fitting, simulations, data prediction

After data acquisition, a number of regions of interest (ROIs) were manually drawn in GM, WM, and in a brain region with voxels dominated by arterial signal (e.g. in the vicinity of the left middle cerebral artery). Mean signal intensity of these ROIs was extracted for all the images acquired.

The NoBS Ss data were fitted using non-linear regression in Prism 3 (GraphPad Software, San Diego California USA, www.graphpad.com) with a conventional 3-parameter saturation recovery curve (fitting for M0, T1, the saturation efficiency α):

$$\mathrm{Ss} = M0 \cdot [1 - \alpha \cdot e^{-T1/T2}] \quad (1)$$

The extracted values (M0, T1, α, $M0_{Sat1/1}$, $T1_{Sat1/1}$, $M0_{Sat1/2}$, $T1_{Sat1/2}$, $M0_{Sat1/3}$, $T1_{Sat1/3}$) were then used to predict the signal behaviour in the BS experiments with and without application of the Q2TIPS pulses.

For this, a simple saturation-plus-double-inversion-recovery computer simulation was set-up with the following properties/assumptions:

1. The initial saturation was calculated according to the measured α (from the fit to Eq. 1).

2. The BS inversions were assumed to be instantaneous and ideal (i.e. transforming the longitudinal magnetisation at time t_k, $M(t_k)^-$ into $M(t_k)^+ = -M(t_k)^-$;
3. The positions of the inversions (t_{BS1}, t_{BS2}) were calculated as in the actual pulse sequence (see the section "Subjects and main MR acquisition protocol", above, or Ref. [14]);
4. The background Ss signal was modelled using:
   (a) the measured M0 and T1 for any time t where $0 < t \leq$ TI1, i.e. from the end of the inversion (labelling) pulse ($t = 0$) to the time of beginning of the Q2TIPS pulse-train; and
   (b) the appropriate $M0_{Sat}$ and $T1_{Sat}$ (according to the chosen Q2TIPS module) for TI1 $< t \leq$ TI;
5. For each interval Δt between times t_k and t_{k+1} the following equation was used:

$$\mathrm{Ss}(t_{k+1}) = M0 \cdot [1 - e^{-\Delta t/\mathrm{T1}}] + \mathrm{Ss}(t_k) \cdot e^{-\Delta t/\mathrm{T1}} \quad (2)$$

with the appropriate M0 and T1 values as described in point 4.

6. The times t_k were: 0, t_{BS1}, t_{BS2}, TI1, and TI in ascending order, defining 4 separate calculation intervals.
7. Flow effects were not modelled.

Assessing the reproducibility of CBF estimates and comparison of results with different Q2TIPS pulse densities

For two subjects (referred to as Subjects I and II), the multi-TI acquisition with TI1 = 500 ms was repeated 5 and 4 times, respectively (in an interleaved fashion), with the conventional Q2TIPS Sat1/1 scheme and the (reduced-MT) Sat1/3 scheme to assess the coefficient of variation (CoV ≡ standard deviation (SD)/mean in percentage units) of the CBF estimates over repeated measures and to compare the perfusion data with simple statistical parameters (mean, SD, *t*-test). All Ss and Ns data from this dataset were realigned (motion corrected) using FSL-FLIRT to the mean of the TI = 900 ms acquisitions from the 1st of the 9 runs. The calculated ΔM values from each run where then smoothed with a 6 mm Gaussian kernel, and FSL-BASIL [20] was used to extract relative CBF values (rCBF, in arbitrary units, au) and BAT, with bolus duration (τ) fixed (equal to TI1) or estimated from the fit. BASIL is a tool for fast Bayesian inference of non-linear models. We used it with the Buxton approach [7] to infer perfusion parameter estimates from multi-TI ASL data. Whole-brain results were visually inspected using percentage change maps for each parameter value estimated from the Sat1/3 data vs. the corresponding parameter value from the Sat1/1 data; for statistical analysis, 3 large cortical ROIs were drawn on each hemisphere on a single slice.

Simulations of an optimised BS scheme accounting for MT-induced variations in M0 and T1

Once the Q2TIPS scheme has been chosen, the MT-induced reduction in M0 and T1 for both GM and WM (i.e. $M0_{Sat}$ and $T1_{Sat}$) can be measured. With this additional information it is then possible to numerically re-calculate the optimum position of the two BS inversion pulses (t_{BS1} and t_{BS2}) to achieve stationary WM and GM signal at all TI values, similar to what would have been obtained in the absence of the MT effect. In this simulation the ROI signal intensities were calculated for a large range of t_{BS1} and t_{BS2} for each TI > TI1; the minimum shifts dt_{BS1}(TI) and dt_{BS2}(TI) (from the values suggested in Ref. [14]) providing a signal similar to the signal obtained for TI < TI1 were selected.

Results

Overall signal intensity pattern when Q2TIPS is used

Figure 1 shows the Ss images of a single slice acquired with BS at all TI values for (a) TI1 = 2,700 ms and (b) TI1 = 1,400 ms for a single representative subject. Row (c) displays the ΔM (Ss − Ns) images for TI1 = 1,400 ms. Whereas in (a) the parenchymal tissue signal is relatively stable even for the longest TI, indicating a well tuned BS scheme, substantial variation in tissue signal intensity is visible in (b) immediately after the start of Q2TIPS (red dashed vertical line): there seems to be a "dip" followed by an "overshoot" of signal intensity. This is a consequence of the deterioration of BS efficiency due to MT effects.

MT-induced reduction in observed T1 and M0

Figure 2 demonstrates how the Q2TIPS schemes with different pulse densities result in reductions of the apparent (a) T1 and (b) M0 for 6 different ROIs (shown in (c)). Averages for 5 subjects are shown for each value, with error bars representing between-subject SD. $M0_{Sat}$ values have been normalised to M0 measured with no Q2TIPS and therefore show the relative reduction in apparent M0 when Q2TIPS pulses are used.

The relative values of $T1_{Sat}$ versus T1 for the 3 Q2TIPS schemes are shown in Table 1. The CoV (mean ± SD) was very low for all variables, indicative of very consistent ROI placement across subjects (e.g. for the GM ROI (pink ROI on slice 11 in (c)) CoV was 5.4 ± 0.2% for M0 and $M0_{Sat}$ and 3.9 ± 0.5% for T1 and $T1_{Sat}$ respectively; for the WM ROI (green ROI on slice 16 in (c)) it was 8.7 ± 0.3 and 1.2 ± 0.3% respectively).

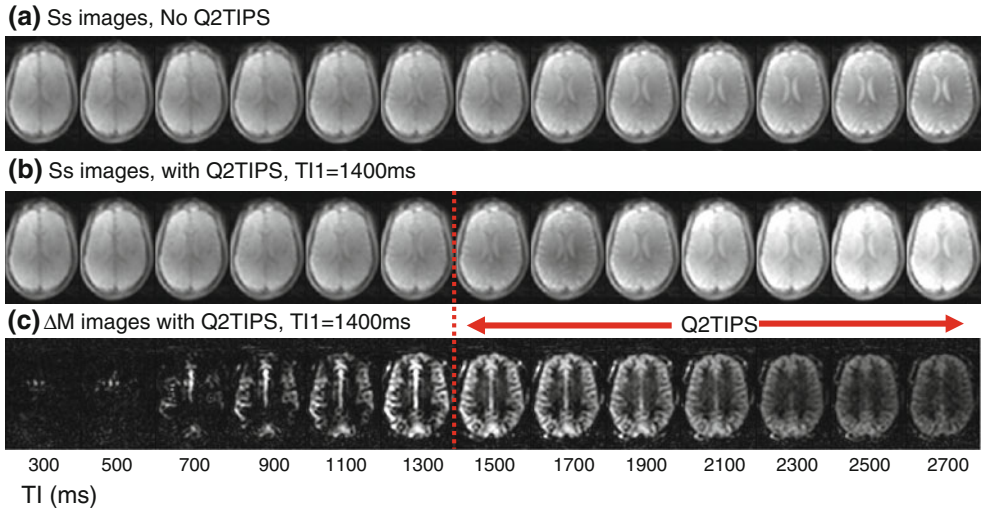

Fig. 1 Slice selective (Ss) images from a single slice of a representative subject at variable inversion times (TI) for: **a** no Q2TIPS; **b** Q2TIPS starting at TI1 = 1,400 ms (indicated by a *vertical red dashed line*). In **c** the difference images ΔM (= Ss − Ns) corresponding to **b** are displayed

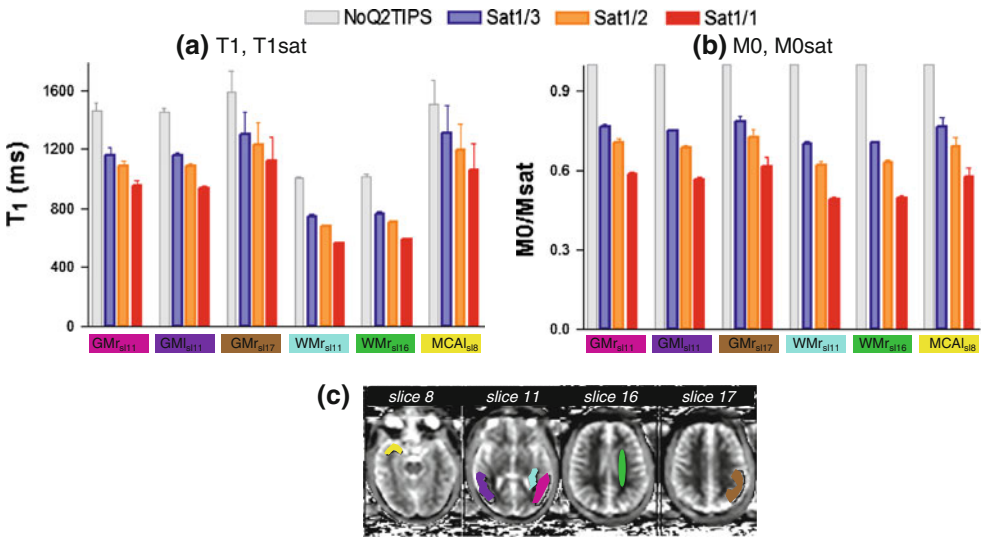

Fig. 2 Q2TIPS results in reductions of apparent T1 (**a**) and M0 (**b**) for the 6 different ROIs shown in **c**: right posterior GM (*pink*, GMr_{sl11}), left posterior GM (*purple*, GMl_{sl11}), right parietal GM (*brown*, GMr_{sl17}), right posterior WM (*cyan*, WMr_{sl11}), right centrum semiovale WM (*green*, WMr_{sl16}), left middle carotid artery (*yellow*, $MCAl_{sl8}$). For each variable the mean and standard deviation for 5 subjects are shown. M0 values have been normalised to M0 measured with no Q2TIPS. *Grey* no Q2TIPS; *blue* Sat1/3, *orange* Sat1/2; *red* Sat1/1 bolus truncation schemes. T1 values normalised for the T1 measured with no Q2TIPS are reported in Table 1

T1 and $T1_{Sat}$ maps of 4 representative slices for one of the subjects are presented in Fig. 3 for (a) no Q2TIPS; (b) Sat1/1, (c) Sat1/2, (d) Sat1/3.

Figure 4 shows measured and predicted (sim) ROI signal intensities from Ss acquisitions scaled by M0 as a function of TI for a variety of acquisition conditions: with no Q2TIPS (a); with the standard (Sat1/1) Q2TIPS scheme and: (b) TI1 = 1,400 ms, (c) TI1 = 1,000 ms, (d) TI1 = 500 ms; for (e)-(f) TI1 = 500 ms and: (e) the Sat1/2 Q2TIPS scheme; (f) the Sat1/3 Q2TIPS scheme.

The average data for 5 subjects for a GM ROI (pink, GMr_{sl11} of Fig. 2) and a WM ROI (green, WMr_{sl16} of Fig. 2) are displayed with SD represented by error bars. This averaging was possible because the ROI placement was extremely consistent between subjects (as indicated by the small error bars).

All curves shown are relatively flat for TI < TI1, indicating consistent BS efficiency; a minimum is then observed (referred to hereafter as "MT-dip") approximately 300 ms after TI1 for TI1 = 1,400 ms and TI1 = 1,000 ms and approximately 200 ms after TI1 for TI1 = 500 ms. The observed changes are a direct result of the changes in M0 and T1 described in Figs. 2, 3 and Table 1.

Table 1 Relative values of $T1_{Sat}$ versus T1 for the three Q2TIPS schemes tested

	GMr_sl11	GMl_sl11	GMr_sl17	WMr_sl11	WMr_sl16	MCAr_sl8
$T1_{Sat1/3}$/T1	0.79 ± 0.01	0.79 ± 0.01	0.82 ± 0.02	0.74 ± 0.01	0.75 ± 0.01	0.87 ± 0.03
$T1_{Sat1/2}$/T1	0.74 ± 0.01	0.74 ± 0.01	0.77 ± 0.04	0.68 ± 0.01	0.70 ± 0.01	0.79 ± 0.04
$T1_{Sat1/1}$/T1	0.65 ± 0.01	0.64 ± 0.01	0.70 ± 0.04	0.56 ± 0.01	0.58 ± 0.01	0.70 ± 0.04

Sat1/1 is the original scheme. In Sat1/2 only every other RF pulse is played out. In Sat1/3 only every third RF pulse has non-zero amplitude

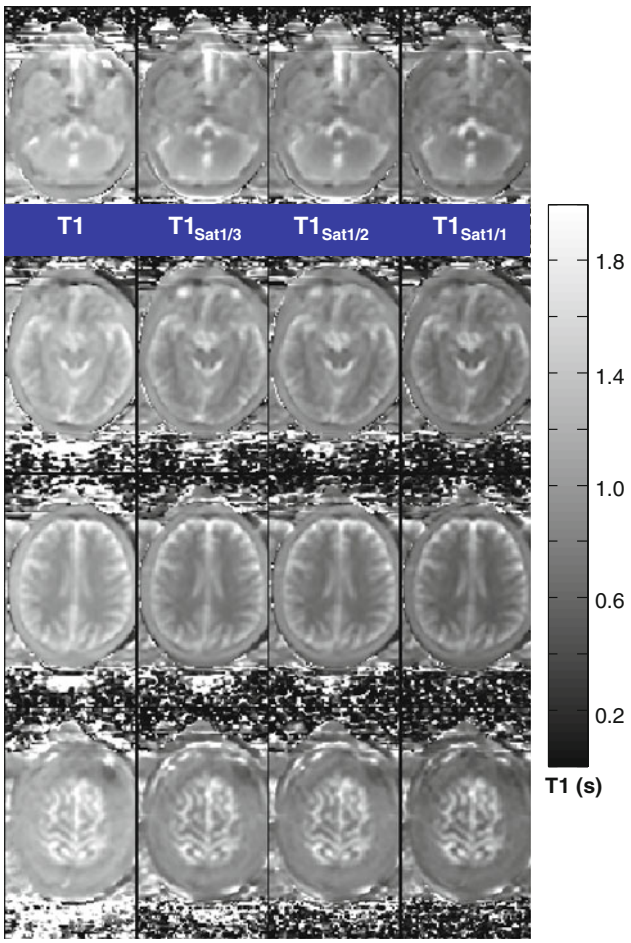

Fig. 3 T1 and $T1_{Sat}$ maps of 4 representative slices for one of the subjects in 4 columns: **a** no Q2TIPS; **b** Sat1/1, **c** Sat1/2, **d** Sat1/3 bolus truncation schemes

From the measured data points and taking the first one (TI = 300 ms) as reference, in the MT-dip the GM (WM) signal is reduced by 8% (25%) for TI1 = 1,400 ms (b), by 10% (23%) for TI1 = 1,000 ms (c), and by 10% (17%) for TI1 = 500 ms (d). The signal intensity of the longest TI (2,700 ms) is above the reference signal in all cases and the maximum signal occurring over all TI values is for GM (WM) 51% (61%) greater than the reference for TI1 = 1,400 ms (b), 43% (54%) greater for TI1 = 1,000 ms (c), and 27% (36%) greater for TI1 = 500 ms (d). In comparison, when no Q2TIPS is used, GM decreases negligibly with TI (2% decrease at TI = 700 ms vs. TI = 300 ms) and then increases slightly (+16% at TI = 2,700 ms). WM decreases very slightly with TI (−5% at TI = 900 ms vs. TI = 300 ms) and then increases slowly not quite reaching its initial value.

Effect of Q2TIPS density on static tissue signal

The effect of reducing the density of the Q2TIPS pulses (or, equivalently, their inter-pulse interval) can be appreciated from Fig. 4d–f. For TI1 = 500 ms we can compare (d) the standard (Sat1/1) Q2TIPS scheme, (e) the Sat1/2 Q2TIPS scheme, and (f) the Sat1/3 Q2TIPS scheme. It is apparent that as the number of pulses per unit time is reduced, the MT-dip becomes shallower and the subsequent overshoot is reduced. Quantitatively, with reference to the TI = 300 ms signal, the measured GM dips are 9.8, 6.4, and 5.4% lower and the maxima 26.7, 19.2, and 14.2% higher, respectively, for Sat1/1, Sat1/2 and Sat1/3. For WM we have −39.1, −34.4, and −33.8% (dips) and 36.1, 24.3, and 17.5% (maxima).

Perfusion signal with the different Q2TIPS schemes

Figure 5 shows the ΔM/M0 data (average for the 5 subjects with SD in error bars) for the 2 ROIs used in Fig. 4. The grey line corresponds to the acquisition without Q2TIPS (NoQ2TIPS); data for TI1 = 1,400 and 1,000 ms are shown in cyan and green respectively; data for TI1 = 500 ms and the 3 different Q2TIPS schemes are in red (Sat1/1), orange (Sat1/2), and blue (Sat1/3); the data with the full density Q2TIPS pulses but no gradients are in pink (NoGrads). Visual inspection of the GM plots reveals two distinct time-courses: when Q2TIPS is used and TI1 = 500 ms the curves appear similar (irrespective of the pulse-train density). Their time-course is markedly different from the time-course of data without Q2TIPS. The averaged NoQ2TIPS and the NoGrads datasets in which Q2TIPS pulses were played out without the appropriate slice selection gradients appear similar. The data with Q2TIPS and TI1 = 1,000 ms or 1,400 ms are also little different from the NoQ2TIPS dataset indicating that for these TI values most of the bolus has already entered the imaging slab. Some small differences between some of the GM curve means seem to be present

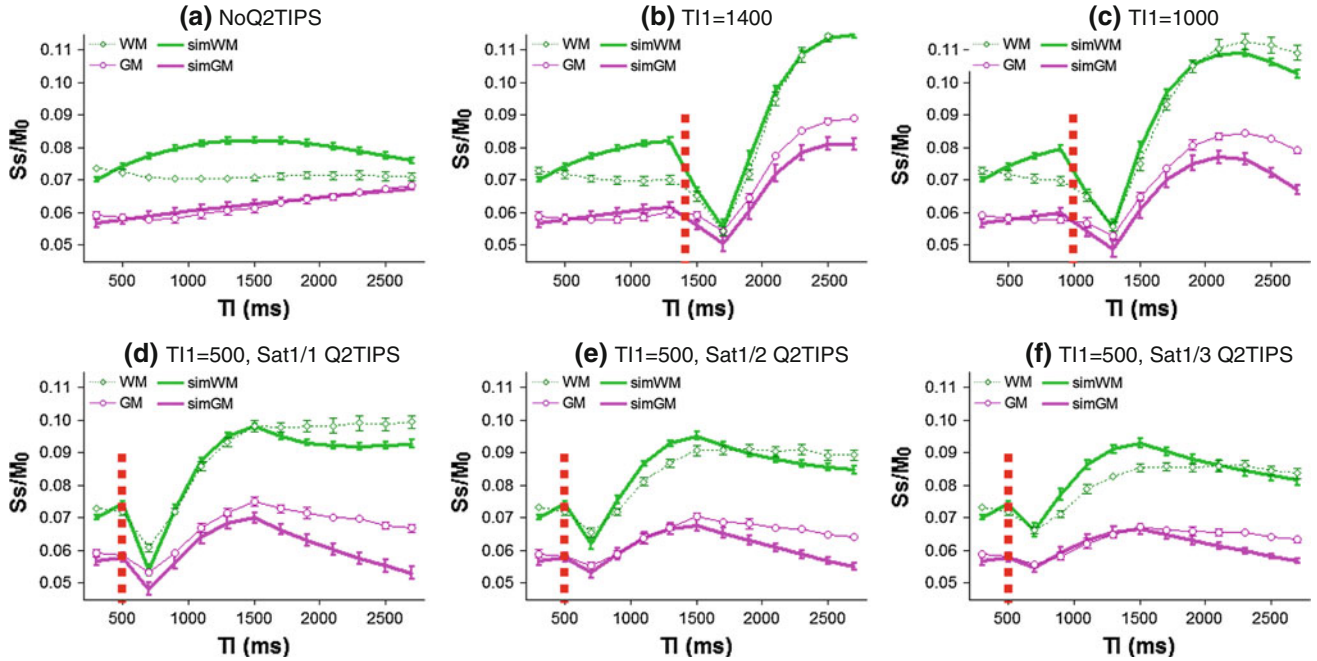

Fig. 4 Measured and predicted (sim) ROI signal intensities normalised by M0 as a function of TI for: **a** No Q2TIPS; **b–d** the standard (Sat1/1) Q2TIPS scheme with **b** TI1 = 1,400 ms, **c** TI1 = 1,000 ms, **d** TI1 = 500 ms; **e**, **f** TI1 = 500 ms and: **e** the Sat1/2 Q2TIPS scheme; **f** the Sat1/3 Q2TIPS scheme. Averages for 5 subjects of the data measured (*diamonds* and *circles*) and simulated (*solid thick lines*) are shown for GM (*pink*, GMr_{sl11} of Fig. 2) and WM (*green*, WMr_{sl16} of Fig. 2) ROIs

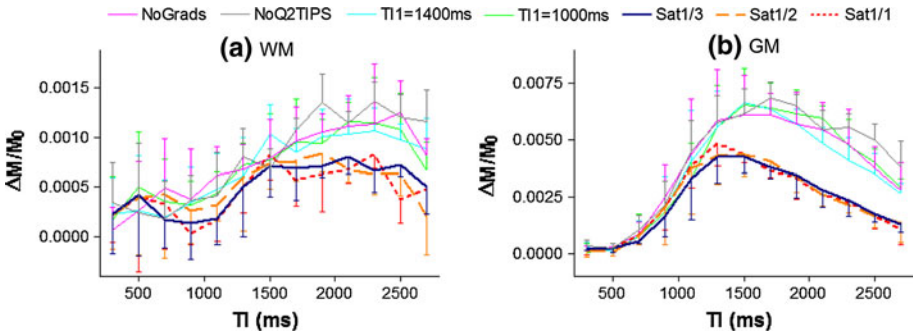

Fig. 5 ΔM/M0 data (mean for 5 subjects) for ROI GMr_{sl11} of Fig. 2 and ROI WMr_{sl16} of Fig. 2 (the same ROIs used in Fig. 4) with *error bars* representing standard deviations. *Grey*, data without Q2TIPS (NoQ2TIPS); *Cyan*, Q2TIPS and TI1 = 1,400 ms; *green*, Q2TIPS and TI = 1,000 ms; *red*, *orange*, and *blue* are for TI1 = 500 ms and the 3 different Q2TIPS schemes: Sat1/1, Sat1/2, Sat1/3, respectively; the *pink lines* labelled NoGrads were measured with Q2TIPS slab-selection gradients turned off

(e.g. for GM the Sat1/1 curve increasing slightly earlier than the Sat1/3 curve and the NoGrads curve appearing slightly lower than the NoQ2TIPS curve); however, the between-subject differences in each ΔM curve were such that no significant differences between the curves were detectable.

Figure 6 shows ΔM data for the 9 runs from the single-subject reproducibility study for the GMr_{sl11} ROI of Fig. 2 (red: Sat1/1; blue: Sat1/3) (subject I). In (b) the means (with SD in error bars) over the multiple runs are plotted separately for the different Q2TIPS schemes. The initial section of the curves for both schemes strongly overlap, whereas at longer TI values the Sat1/1 curve is lower than the Sat1/3 curve, reflecting the signal reduction caused by the Q2TIPS-related MT effect. The asymmetric nature of this effect results in the Sat1/3 curve (blue) appearing slightly wider than the Sat1/1 curve (red). The curves from subject II had the same characteristics (data not shown).

Perfusion parameter estimates with the different Q2TIPS schemes

The perfusion parameters estimates from FSL-BASIL are reported for 2 subjects on the 6 ROIs shown in Fig. 7. Values in Tables 2a and 3a are for the simplest model with fixed bolus duration; values in Tables 2b and 3b are for the

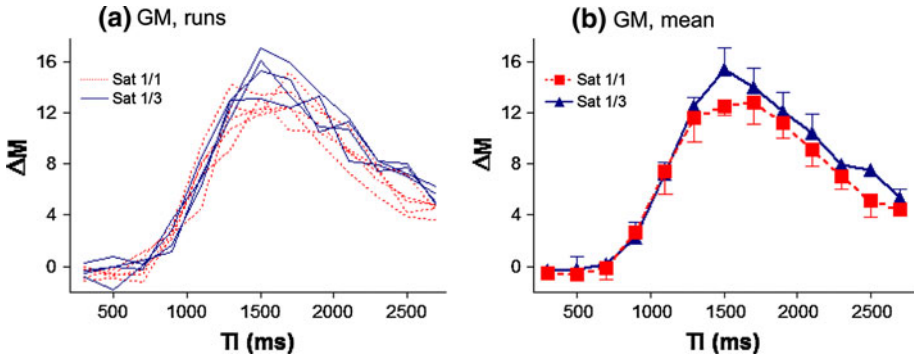

Fig. 6 ΔM data for the separate runs of the reproducibility study for a GM ROI equivalent to GMr_{sl11} (also used in Figs. 4, 5) for the original Q2TIPS scheme Sat1/1 (*red*, *dashed*) and the Sat1/3 scheme (*blue*, *continuous lines*) in **a**. In **b** the means for the multiple runs from each Q2TIPS approach are plotted with error bars representing standard deviations. *Red* Sat 1/1; *blue* Sat1/3

model which includes fitting of τ. Reproducibility across the multiple repeats was satisfactory. Using the simpler 2-parameter model, averaging over the 6 ROIs and the 2 subjects, the mean (±SD) CoVs were 5 ± 2 and 6 ± 1% for rCBF and 4 ± 2 and 3 ± 1% for BAT for Sat1/1 and Sat1/3 Q2TIPS schemes respectively (Tables 2a, 3a). For the model involving fitting of τ the CoV were 7 ± 4 and 10 ± 4% for rCBF, 4 ± 2 and 4 ± 1% for BAT and 6 ± 3 and 8 ± 4% for τ (Sat1/1 and Sat1/3 Q2TIPS schemes respectively) (Tables 2b, 3b).

On visual inspection of percentage change maps of perfusion parameter estimates (not shown), the most consistent observation is that for both subjects the Sat1/3 scheme gives rCBF estimates larger than the Sat1/1 scheme almost everywhere across the brain for the 2-parameter model. For the 3-parameter model, in a few areas, especially the inferior parietal and temporal lobes, this increase is not as consistent. For subject I, for the 2-parameter fit, BAT appears slightly prolonged, and for the 3-parameter fit there is an indication of increased τ in some temporal and parietal regions.

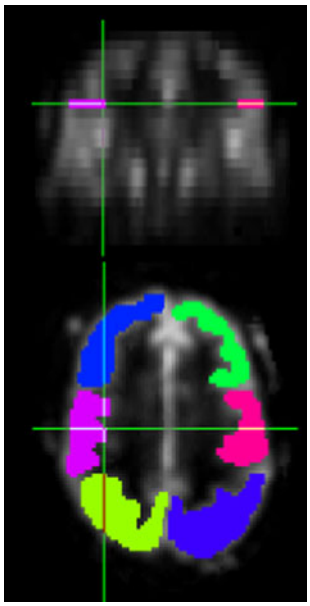

Fig. 7 The 6 ROIs used to evaluate perfusion parameters extracted from data acquired with Sat1/1 and Sat1/3 Q2TIPS schemes are shown superimposed on a mean rCBF map calculated with FSL-BASIL in coronal and axial views for Subject I. ROIs for Subject II were analogous

In Tables 2 and 3 the *t*-test (unpaired, 1 tailed, unequal variance) *P*-values are denoted by an asterisk when $P \leq 0.05$. When using the 2-parameter model, significant differences between rCBF estimated for the two Q2TIPS schemes were observed for all ROIs, with the Sat 1/3 scheme resulting in a higher estimated rCBF (range 6–15%, mean difference 10 ± 2% (Subject I) or range 8–11%, mean difference 10 ± 1% (subject II)). For subject I the BAT values also appear significantly higher in 3 ROIs for the Sat 1/3 Q2TIPS scheme (overall range 2–7%, mean difference 3.5 ± 2.0%) whereas no large or statistically significant difference appears for subject II.

When τ is explicitly fitted within the model some of the differences in rCBF lose their significance: all occipital rCBF differences remain significant (approximately 12% for both subjects); subject II also retains differences in the frontal ROIs, 13.6 (left, $P = 0.03$) and 12.3% (right, trend: $P = 0.057$). The BAT differences for subject I also lose their significance (overall range −2 to 3%, mean difference 1.6 ± 2.0%) when τ is fitted; in 2 ROIs of subject I (right frontal and parietal) the significant differences previously seen in rCBF appear to shift to τ (mean subject I τ is 540 ± 60 ms for Sat1/1 and 570 ± 40 ms for Sat1/3, whereas the "ideal" τ (user defined TI1) is 500 ms); presumably, in these cases, once τ is allowed to vary (and be fitted), the Sat1/3 time-courses fit better with a τ value longer than TI1, whereas CBF and BAT become more similar to their Sat1/1 value. These ROI results seem to be representative of the findings over the whole brain.

Modification of the BS scheme taking into account MT effects

Figure 8 shows simulated examples of dip-plus-overshoot for GM and WM resulting from Q2TIPS-related MT reduction in T1 and M0 (red curves; see caption for ROI relaxation times used). This deterioration of the BS scheme

Table 2 Perfusion parameter estimates from FSL-BASIL for subject I

	rCBF (au)				BAT (s)			
	Sat 1/1	Sat1/3	%diff	*P*	Sat 1/1	Sat1/3	%diff	*P*
(a)								
occGMl	19.1 ± 1.7	21.3 ± 1.5	11.4	0.038*	0.94 ± 0.03	0.96 ± 0.03	2.2	0.176
occGMr	22.1 ± 1.5	25.4 ± 1.4	14.6	0.006*	0.92 ± 0.01	0.95 ± 0.02	3.3	0.034*
parGMl	18.8 ± 1.2	20.1 ± 0.7	7.3	0.039*	0.70 ± 0.01	0.76 ± 0.02	7.3	0.007*
parGMr	23.1 ± 0.5	24.6 ± 1.0	6.5	0.024*	0.59 ± 0.01	0.60 ± 0.03	1.8	0.247
fGMl	27.4 ± 2.6	30.1 ± 1.6	10.1	0.047*	0.84 ± 0.02	0.87 ± 0.02	3.9	0.010*
fGMr	30.2 ± 2.2	33.6 ± 1.9	11.4	0.020*	0.88 ± 0.02	0.90 ± 0.02	2.6	0.091

	rCBF (au)				BAT (s)				τ (s)			
	Sat 1/1	Sat1/3	%diff	*P*	Sat 1/1	Sat1/3	%diff	*P*	Sat 1/1	Sat1/3	%diff	*P*
(b)												
occGMl	18.5 ± 1.9	20.9 ± 1.3	12.7	0.030*	0.92 ± 0.03	0.95 ± 0.04	2.3	0.192	0.56 ± 0.03	0.56 ± 0.01	1.0	0.352
occGMr	21.5 ± 1.5	23.9 ± 1.4	11.0	0.022*	0.90 ± 0.01	0.93 ± 0.03	2.7	0.120	0.57 ± 0.02	0.57 ± 0.03	1.2	0.374
parGMl	20.5 ± 1.3	19.6 ± 2.0	−4.4	0.232	0.71 ± 0.01	0.74 ± 0.04	3.1	0.170	0.48 ± 0.03	0.55 ± 0.07	13.9	0.071
parGMr	26.2 ± 0.8	25.8 ± 2.4	−1.5	0.389	0.61 ± 0.01	0.60 ± 0.04	−1.8	0.287	0.45 ± 0.02	0.51 ± 0.04	12.1	0.026*
fGMl	26.5 ± 3.0	27.8 ± 1.5	4.8	0.216	0.82 ± 0.02	0.84 ± 0.02	2.9	0.061	0.56 ± 0.02	0.58 ± 0.02	2.1	0.226
fGMr	27.0 ± 1.8	27.8 ± 1.6	2.9	0.258	0.85 ± 0.02	0.85 ± 0.03	0.5	0.414	0.59 ± 0.02	0.64 ± 0.03	8.6	0.021*

Relative CBF (rCBF, in arbitrary units, au) and bolus arrival time (BAT, in seconds) in Table 2a were obtained assuming fixed bolus duration (τ) equal to TI1. Data in Table 2b were obtained allowing for fitting of τ (in seconds). ROIs can be seen in Fig. 7; they are labelled "l" or "r" for left and right, hemispheres respectively; regional labels are: *occGM* occipital GM; *parGM* parietal GM; *fGM* frontal GM

* $P \leq 0.05$

Table 3 Perfusion parameter estimates from FSL-BASIL for subject II

	rCBF (au)				BAT (s)			
	Sat 1/1	Sat1/3	%diff	*P*	Sat 1/1	Sat1/3	%diff	*P*
(a)								
occGMl	17.7 ± 0.6	19.5 ± 1.1	10.4	0.008*	0.92 ± 0.05	0.92 ± 0.02	−0.6	0.415
occGMr	19.1 ± 0.6	21.1 ± 1.5	10.5	0.017*	0.93 ± 0.03	0.91 ± 0.03	−2.0	0.171
parGMl	19.6 ± 0.4	21.2 ± 1.4	8	0.032*	0.67 ± 0.05	0.69 ± 0.01	1.8	0.304
parGMr	20.5 ± 1.3	22.4 ± 1.3	9.3	0.024*	0.59 ± 0.04	0.61 ± 0.01	4.2	0.134
fGMl	22.8 ± 1.0	24.9 ± 1.7	9.1	0.025*	0.91 ± 0.04	0.90 ± 0.03	−1.7	0.253
fGMr	25.0 ± 1.3	27.3 ± 1.9	9.6	0.028*	0.90 ± 0.04	0.88 ± 0.02	−2.1	0.210

	rCBF (au)				BAT (s)				τ (s)			
	Sat 1/1	Sat1/3	%diff	*P*	Sat 1/1	Sat1/3	%diff	*P*	Sat 1/1	Sat1/3	%diff	*P*
(b)												
occGMl	17.9 ± 1.0	20.0 ± 2.0	12.1	0.037*	0.91 ± 0.05	0.91 ± 0.02	−0.2	0.469	0.55 ± 0.04	0.53 ± 0.04	−2.1	0.323
parGMl	19.8 ± 2.4	20.6 ± 3.7	4.1	0.348	0.66 ± 0.05	0.66 ± 0.03	0.4	0.460	0.55 ± 0.07	0.57 ± 0.07	2.8	0.366
fGMl	20.6 ± 0.5	23.2 ± 2.8	12.3	0.057	0.88 ± 0.05	0.87 ± 0.02	−1.0	0.357	0.61 ± 0.04	0.59 ± 0.05	−3.3	0.251
occGMr	20.4 ± 0.5	22.8 ± 2.1	11.8	0.031*	0.93 ± 0.03	0.91 ± 0.04	−1.5	0.283	0.53 ± 0.04	0.51 ± 0.03	−3.7	0.191
parGMr	23.2 ± 3.5	22.9 ± 4.1	−14	0.449	0.60 ± 0.05	0.61 ± 0.03	0.7	0.442	0.47 ± 0.05	0.52 ± 0.07	11.1	0.113
fGMr	22.7 ± 1.3	25.8 ± 2.7	13.6	0.030*	0.86 ± 0.04	0.85 ± 0.02	−0.7	0.394	0.62 ± 0.03	0.57 ± 0.05	−6.8	0.079

Relative CBF (rCBF, in arbitrary units, au) and bolus arrival time (BAT, in seconds) in Table 3a were obtained assuming fixed bolus duration (τ) equal to TI1. Data in Table 3b were obtained allowing for fitting of τ (in seconds). ROIs were analogous to those shown in Fig. 7 for subject I; they are labelled "l" or "r" for left and right hemispheres respectively; regional labels are: *occGM* occipital GM, *parGM* parietal GM, *fGM* frontal GM

* $P \leq 0.05$

can be avoided by calculating for TI > TI1 some ad-hoc shifts in the positions (t_{BS1} and t_{BS2}) of the BS pulses that take into account MT effects (blue curves). Table 4 shows for each TI > TI1 the original t_{BS1} and t_{BS2} and the new positions that simultaneously stabilise the signals of GM and WM in Fig. 8: $t_{BS1} + dt_{BS1}$ and $t_{BS2} + dt_{BS2}$.

Discussion

The data presented here clearly demonstrate an issue related to the application of Q2TIPS that, as far as the authors are aware, has not been previously discussed in the ASL literature.

The saturation pulse train necessary for Q2TIPS is equivalent, for both tissue and blood in the imaging slab, to the off-resonance pulses used to generate contrast in magnetisation transfer MRI. This MT effect increases with amplitude and density of the Q2TIPS pulses.

The first consequence of the Q2TIPS-related MT effect is that for long inversion times when TI > TI1 (i.e. after the Q2TIPS pulse train has started) the apparent T1 and M0 of tissue decrease (we have called these $T1_{Sat}$ and $M0_{Sat}$). Such an effect can be clearly seen in Table 1, the bar-plots of Fig. 2, and the T1 and $T1_{Sat}$ maps in Fig. 3: the greater the pulse density, the greater the MT effect, and, hence, the greater the reduction in T1 and M0.

The position of the BS inversion pulses is optimised for a specific pair of T1 values, typically corresponding to WM and GM T1, and effective static tissue suppression is based on the assumption that M0 and T1 remain stationary over the interval (TI) between the labelling pulse and the readout. The reduction in T1 and M0 thus leads to a reduced efficacy of the background-suppression scheme, and the observed signal behaviour of the ASL base images (Ss and Ns) can be explained by this MT-induced T1-shortening.

We have shown (Figs. 1a, 4a) that when Q2TIPS is not used, WM intensity in background tissue is approximately stable whereas GM increases only slightly for the longer TI values.

When the Q2TIPS module is introduced there is a signal intensity "dip" occurring 200–300 ms post TI1, followed by an increase for all tissues types (Figs. 1b, 4b–d).

The main problem with the reduced efficacy of the BS of the static signal is that the relatively small perfusion signal difference (ΔM) becomes less precise as it is more affected by physiological noise in the tissue signal plus potential subject motion. Moreover, this happens exactly for intermediate to long TI values, which is when most of the perfusion signal appears.

We have measured an increase of up to ~27 (GM ROI) and 36% (WM ROI) in the background signal for the longest TI here employed. Any non-perfusion-related change in tissue signal will thus be amplified by these factors and the resulting temporal stability will correspondingly decrease [9].

The MT-dip produced by the Q2TIPS pulses can be easily modelled by using a simple saturation-plus-double-inversion-recovery simulation using the measured M0, T1, $M0_{Sat}$, and $T1_{Sat}$, and the simulations are in good qualitative agreement with the measured data. There is a remaining small discrepancy between simulated and real data, mostly in the intermediate TI values for WM and the longest TI for GM; this is likely to be because the simulation neglected flow effects and assumed that all pulses were instantaneous. The effect of reducing the efficiency of the inversion pulses was investigated, but the differences between the results were negligible; this is because reduced efficiency of the 1st inversion pulse leads to higher magnetisation before the 2nd inversion pulse and this extra magnetization is lost almost entirely because of the reduced efficiency of this 2nd pulse (data not shown).

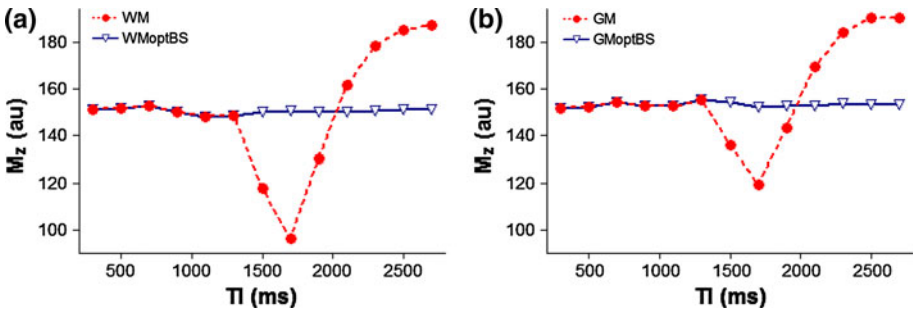

Fig. 8 Simulation data showing that it is possible to modify the BS scheme to take into account MT effects. When the conventional 2-inversion pulses BS scheme is used, Q2TIPS-related MT-induced reductions in T1 and M0 produce an "MT-dip" plus overshoot (*red*). If the position of BS pulses (t_{BS1} and t_{BS2}) are adjusted to account for MT effects the static tissue signal intensity can be stabilised even at TI > TI1 for WM and GM simultaneously (*blue*, "optBS" labels). **a** WM: M0 = 1,609, $M0_{Sat}$ = 0.492·M0, T1 = 1,011 ms, $T1_{Sat}$ = 0.584·T1; **b** GM: M0 = 2,303, $M0_{Sat}$ = 0.576·M0, T1 = 1,464 ms, $T1_{Sat}$ = 0.643·T1. TI1 was 1,400 ms and t_{BS1} and t_{BS2} were only modified for TI > TI1. The original timing t_{BS1} and t_{BS2}, and the optimised timings $t_{BS1} + dt_{BS1}$ and $t_{BS2} + dt_{BS2}$ used for each TI are listed in Table 4

Table 4 Optimised inversion pulses timings for adjusted BS scheme enabling compensation of MT effects

TI	t_{BS1}	t_{BS2}	$t_{BS1} + dt_{BS1}$	$t_{BS2} + dt_{BS2}$
1,500	500	1,159	430	1,107
1,700	599	1,339	471	1,247
1,900	705	1,521	625	1,467
2,100	818	1,705	812	1,711
2,300	937	1,891	961	1,919
2,500	1,064	2,079	1,096	2,113
2,700	1,197	2,268	1,237	2,304

TI1 = 1,400 ms, so only data for TI > TI1 are shown. t_{BS1} and t_{BS2} are the calculated positions of the 2 BS inversion pulses at each TI according to Ref. [14]; $t_{BS1} + dt_{BS1}$ and $t_{BS2} + dt_{BS2}$ represent the new positions necessary to simultaneously stabilise signals of GM and WM (assuming relaxation times defined in the caption of Fig. 8) once Q2TIPS-related MT effects are accounted for. All values are in ms

To further verify that the observed change in T1 and M0 is caused by MT, we collected a dataset in which Q2TIPS was applied with no slice selection gradients: the T1 and M0 reduction was exactly the same as for the correct Q2TIPS implementation (within 2% for T1 and 3% for M0) demonstrating that the MT associated with the NoGrads experiment is the same as for the experiment with Q2TIPS (data not shown).

We have artificially modulated the Q2TIPS-related MT effect by reducing the density of RF pulses in the Q2TIPS pulse train by a factor of 2 and 3. In our experimental setting this could be done while keeping the cut-off velocity above 93 cm/s, thus ensuring the trailing end of the bolus is still efficiently truncated. For instance, for the main GM ROI analysed, the T1 reduction was 35% for the original Sat1/1 scheme, 26% for Sat1/2, and 21% for Sat1/3; the corresponding M0 reductions were 42, 30, and 24% respectively (Table 1). As a consequence, comparing Fig. 4d and f we can see that the amplitude of the MT-dip and the subsequent overshoot for the Ss data are substantially reduced when using the Sat1/3 scheme.

Additionally, to reduce the overall power of the Q2TIPS pulse train it is possible to reduce its duration by ending it at a time $TI1_{Sat}$ sometime before TI ($TI1 < TI1_{Sat} < TI$) as described elsewhere [3, 21].

It has been demonstrated through simulations that the MT-dip in the background tissue signal can be avoided and a stationary Ss or Ns signal can be maintained: this is possible by re-adjusting the position of the BS pulses according to the measured Q2TIPS-induced MT effect on M0 and T1 for both GM and WM (Fig. 8). The BS scheme used here was optimised for tissues with T1 values in the ratio 2:1, because in this case a simple analytical expression for the position of the inversion pulses can be found [14]. The T1 values of GM and WM at 3T have a ratio closer to 1.5:1 and we explored with simulations the effect of optimising the BS scheme for this ratio. Although the stability of the simulated WM signal at long TI values improves slightly, there is no qualitative or appreciable quantitative change in the signal behaviour and description of the Q2TIPS-induced MT effect.

It is, however, also important to keep in mind that while the background tissue signal level at the time of the excitation pulses (and thus the sensitivity to undesired temporal instabilities of the ASL sequence) can be maintained constant by shifting the BS pulses, the actual MT effect in tissue and blood (and the consequences on perfusion quantification) is not affected by the position of the BS pulses.

We have fully modelled the MT effect of the Q2TIPS pulses on the background tissue signal. However, perfused tissue and labelled blood will also be affected; this will affect the actual perfusion signal and consequently CBF estimation. This effect is more complex to model, because the tagged blood spins (characterised by $M0_{blood}$, $M0_{Sat}^{blood}$, $T1^{blood}$, $T1_{Sat}^{blood}$) can exchange with tissue spins (M0, $M0_{Sat}$, T1, $T1_{Sat}$) at different times relative to the FAIR inversion pulse, and these timings depend on brain region. However, it is important to note that the MT effect in blood is less significant than in tissue [22, 23].

It would be possible to measure the MT effect on blood with methods such as those described elsewhere [24, 25] and then fit for a variable exchange time between blood and tissue when modelling the signal behaviour, e.g. by an extension of Buxton model [7]. Signal-to-noise issues may complicate this modelling with real data, but this avenue remains to be explored in the future.

To quantify how the Q2TIPS-related MT effect affected the perfusion (ΔM) signal in our set up, the data shown in Fig. 5 could be used (comparing the ΔM signals from the NoGrads vs. No Q2TIPS acquisitions or the 3 Q2TIPS schemes). However, it was soon evident that relatively large between-subject differences (due to individual anatomy differences) prevented such analysis.

Therefore a preliminary assessment of how much the Q2TIPS-related MT effect can affect the perfusion signal and CBF quantification was carried out using data collected for 2 subjects for which several acquisitions using different saturation schemes were alternated in rapid succession. Analysis using the Buxton model [7] as implemented in FSL-BASIL [20] showed that calculated rCBF values were underestimated by up to 15% in the MT-"heavy" acquisition versus the lighter-MT acquisition (and would most likely be greater if it were possible to measure CBF in complete absence of MT effects).

Moreover, the way the ASL signal is modelled had a significant effect on the result and the magnitude of the resulting error. Using a simple 2-parameter fit (assuming

the experimentally defined bolus duration $\tau = TI1$), MT-related rCBF reduction was observed for most of the brain and was statistically significant in all ROIs for both subjects.

When the bolus duration τ was also fitted, in some brain regions these rCBF differences decreased. For one of the subjects, an estimated τ significantly increased for the acquisition with the fewest saturation pulses was observed for 2 out of 6 ROIs.

One explanation for this estimated τ increase in some regions could be that the saturation scheme with reduced density of Q2TIPS pulses was not as efficient in saturating the bolus as the higher-density scheme. The cut-off velocity calculations for our Q2TIPS schemes would indicate this is a small effect; the possibility of a contribution of reduced bolus-truncation efficiency to the signal differences here presented cannot, however, be completely excluded.

The observed decrease in ΔM and reduction in estimated rCBF here attributed to MT is consistent with what would be described by the Buxton model (equation 2 in Ref. [7]) assuming that once water reaches a voxel and exchanges into the tissue the magnetisation decays with a reduced T1sat rather than the original tissue T1; this is true even when neglecting MT effects in blood and without assuming that the tagged water exchanges immediately into the tissue (the common assumption of exchange time, $Tex = 0$; larger Tex means the effect starts to appear later).

The simple 2-parameter fit, not taking into account the demonstrated MT-induced decrease in tissue T1 and M0, results in a model that is slightly inaccurate, leading to a reduction of estimated rCBF (and, in one of the subjects, BAT).

The decrease in τ in some ROIs can also be similarly explained. When τ is allowed to change in the 3-parameter fit (still not taking into account MT effects) it is natural that some of the discrepancy between the model and the data may be absorbed by τ, especially because, although changes in T1 and τ appear clearly different on noiseless numerical simulations, their effects may be hard to distinguish in low-SNR in-vivo data.

Tissue T1 can also be fitted within FSL-BASIL. However for the purposes of this paper it was more appropriate to assume a fixed T1, use the simplest models conventionally employed, and observe the resulting effect on estimated rCBF.

As mentioned above, the perfusion model should be more substantially modified to account for the observed changes in tissue T1 and measured or estimated changes in blood T1 should help recover an estimate or rCBF unaffected by Q2TIPS-induced MT effect.

Although our analysis was performed on multi-TI ASL, the same observations are valid for any single-TI ASL protocol, with the additional issue that there are many more assumptions that are made to achieve a quantitative CBF estimation and the full kinetic model cannot be fitted to the data. It is thus expected that for single-TI acquisitions the bias introduced by the MT effect would depend on the chosen values of TI and TI1 and could be even greater than shown here.

Conclusions

We have demonstrated for the first time that Q2TIPS pulses have a significant MT effect which reduces tissue T1 and M0. One consequence of this is a reduced BS efficiency for the ASL sequence. However the BS scheme can be re-optimised by taking into account these MT-related T1 and M0 changes. In addition, rCBF estimates made using standard models which do not account for this Q2TIPS-related MT effect can be significantly reduced. We have shown that one way to minimise the MT effect is by reducing the density of the Q2TIPS pulse train.

It is recommended that MT effects of Q2TIPS pulse trains are characterised and CBF quantification models modified accordingly.

Acknowledgments The authors thank all the volunteers that gave their time for this project. Special thanks to Dr Michael Chappell from the FMRIB in Oxford for providing the authors with a version of FSL-BASIL before its public release, with documentation on its use. We also thank the paper reviewers for their useful comments and suggestions. This work was undertaken at University College London Hospitals/University College London, which received a proportion of funding from the Department of Health's National Institute for Health Research Comprehensive Biomedical Research Centre funding scheme. The Collaboration between M.G and UCL was facilitated by European COST Action BM1103 on "Arterial spin labelling Initiative in Dementia (AID)". M.G. was in part funded by the German Ministry of Education and Research (BMBF) under grant number 01EV0702.

References

1. Petersen ET, Mouridsen K, Golay X, all named co-authors of the QUASAR test-retest study (2010) The QUASAR reproducibility study, Part II: results from a multi-center Arterial Spin Labeling test-retest study. Neuroimage 49(1):104–113
2. Wong EC, Buxton RB, Frank LR (1998) Quantitative imaging of perfusion using a single subtraction (QUIPSS and QUIPSS II). Magn Reson Med 39(5):702–708
3. Luh WM, Wong EC, Bandettini PA, Hyde JS (1999) QUIPSS II with thin-slice TI1 periodic saturation: a method for improving accuracy of quantitative perfusion imaging using pulsed arterial spin labeling. Magn Reson Med 41(6):1246–1254
4. Günther M, Bock M, Schad LR (2001) Arterial spin labeling in combination with a look-locker sampling strategy: inflow turbo-sampling EPI-FAIR (ITS-FAIR). Magn Reson Med 46(5):974–984
5. Petersen ET, Lim T, Golay X (2006) Model-free arterial spin labeling quantification approach for perfusion MRI. Magn Reson Med 55(2):219–232

6. MacIntosh BJ, Filippini N, Chappell MA, Woolrich MW, Mackay CE, Jezzard P (2010) Assessment of arterial arrival times derived from multiple inversion time pulsed arterial spin labeling MRI. Magn Reson Med 63(3):641–647
7. Buxton RB, Frank LR, Wong EC, Siewert B, Warach S, Edelman RR (1998) A general kinetic model for quantitative perfusion imaging with arterial spin labeling. Magn Reson Med 40(3): 383–396
8. MacIntosh BJ, Pattinson KT, Gallichan D, Ahmad I, Miller KL, Feinberg DA, Wise RG, Jezzard P (2008) Measuring the effects of remifentanil on cerebral blood flow and arterial arrival time using 3D GRASE MRI with pulsed arterial spin labelling. J Cereb Blood Flow Metab 28(8):1514–1522
9. Ye FQ, Frank JA, Weinberger DR, McLaughlin AC (2000) Noise reduction in 3D perfusion imaging by attenuating the static signal in arterial spin tagging (ASSIST). Magn Reson Med 44(1): 92–100
10. Wong EC, Buxton RB, Frank LR (1998) A theoretical and experimental comparison of continuous and pulsed arterial spin labeling techniques for quantitative perfusion imaging. Magn Reson Med 40(3):348–355
11. Golay X, Hendrikse J, Lim TC (2004) Perfusion imaging using arterial spin labeling. Top Magn Reson Imaging 15(1):10–27
12. Kim SG (1995) Quantification of relative cerebral blood flow change by flow-sensitive alternating inversion recovery (FAIR) technique: application to functional mapping. Magn Reson Med 34(3):293–301
13. Kwong KK, Belliveau JW, Chesler DA, Goldberg IE, Weisskoff RM, Poncelet BP, Kennedy DN, Hoppel BE, Cohen MS, Turner R et al (1992) Dynamic magnetic resonance imaging of human brain activity during primary sensory stimulation. Proc Natl Acad Sci USA 89(12):5675–5679
14. Günther M, Oshio K, Feinberg DA (2005) Single-shot 3D imaging techniques improve arterial spin labeling perfusion measurements. Magn Reson Med 54(2):491–498
15. Griswold MA, Jakob PM, Heidemann RM, Nittka M, Jellus V, Wang J, Kiefer B, Haase A (2002) Generalized autocalibrating partially parallel acquisitions (GRAPPA). Magn Reson Med 47:1202–1210
16. Golay X, Petersen ET, Hui F (2005) Pulsed star labeling of arterial regions (PULSAR): a robust regional perfusion technique for high field imaging. Magn Reson Med 53(1):15–21
17. Ordidge RJ, Wylezinska M, Hugg JW, Butterworth E, Franconi F (1996) Frequency offset corrected inversion (FOCI) pulses for use in localized spectroscopy. Magn Reson Med 36(4):562–566
18. Lu H, Nagae-Poetscher LM, Golay X, Lin D, Pomper M, van Zijl PC (2005) Routine clinical brain MRI sequences for use at 3.0 Tesla. J Magn Reson Imaging 22(1):13–22
19. Wong EC, Buxton RB, Frank LR (1997) Implementation of quantitative perfusion imaging techniques for functional brain mapping using pulsed arterial spin labeling. NMR Biomed 10(4–5):237–249
20. Chappell MA, Groves AR, Whitcher B, Woolrich MW (2009) Variational Bayesian inference for a non-linear forward model. IEEE Trans Signal Process 57(1):223–236
21. Gallichan D, Jezzard P (2009) Variation in the shape of pulsed arterial spin labeling kinetic curves across the healthy human brain and its implications for CBF quantification. Magn Reson Med 61(3):686–695
22. Hernandez-Garcia L, Lewis DP, Moffat B, Branch CA (2007) Magnetization transfer effects on the efficiency of flow-driven adiabatic fast passage inversion of arterial blood. NMR Biomed 20(8):733–742
23. Pike GB, Hu BS, Glover GH, Enzmann DR (1992) Magnetization transfer time-of-flight magnetic resonance angiography. Magn Reson Med 25(2):372–379
24. Thomas DL, Lythgoe MF, Gadian DG, Ordidge RJ (2006) In vivo measurement of the longitudinal relaxation time of arterial blood (T1a) in the mouse using a pulsed arterial spin labeling approach. Magn Reson Med 55(4):943–947
25. Varela M, Hajnal JV, Petersen ET, Golay X, Merchant N, Larkman DJ (2011) A method for rapid in vivo measurement of blood T1. NMR Biomed 24(1):80–88